

Robert Sjöback
Jan Nygren
Mikael Kubista
Department of Biochemistry
and Biophysics,
Chalmers University
of Technology,
S-413 90 Göteborg, Sweden

Received 20 January 1998;
accepted 2 June 1998

Characterization of Fluorescein–Oligonucleotide Conjugates and Measurement of Local Electrostatic Potential

Abstract: The properties of fluorescein are substantially altered upon conjugation to nucleic acids, affecting not only the molar absorptivities and fluorescence quantum yields but also the protolytic equilibrium constant and fluorescence lifetimes. Around neutral pH, the fluorescein moiety is present as both mono- and dianion, and the pK_a relating them is increased from 6.43 for free fluorescein to about 6.90 for fluorescein attached to both single- and double-stranded oligonucleotides of at least 12 bases/base pairs. This difference reflects the local electrostatic potential around the nucleic acid, which is calculated to -28 mV. The molar absorptivities and spectral responses of the conjugated fluorescein protolytic species are also determined, from which the concentrations of fluorescein–oligonucleotide conjugates can be calculated by assuming: $\epsilon_{494} = 62000/[1 + 10^{-(pH-6.90)}] + 12000/[1 + 10^{(pH-6.90)}]$ ($M^{-1} cm^{-1}$). The fluorescence quantum yield of the conjugates depends, in a complex way, on temperature, environment and oligonucleotide length, sequence and conformation, and must be determined for each experimental situation. © 1998 John Wiley & Sons, Inc. Biopoly 46: 445–453, 1998

Keywords: fluorescein–oligonucleotide conjugates; local electrostatic potential; local pH; protolytic equilibrium; FITC fluorescence energy transfer; dye labeled oligonucleotides

INTRODUCTION

One of the most commonly used fluorescent dyes today is fluorescein. It has a very high molar absorptivity in the visible region, a large fluorescence quantum yield, and a high photostability, which makes it very useful in applications where a high sensitivity is needed. Furthermore, it is commercially available in many derivatives, like fluorescein isothiocyanate and fluorescein succinimidyl ester, which can be covalently attached to macromolecules and amino acids. Therefore, fluorescein derivatives are frequently used

in studies of nucleic acids and proteins. Together with, for example, tetramethyl-rhodamine, it can be used in energy transfer measurements to determine distances within and between molecules.¹ Fluorescein is also used to label macromolecules for detection in, for example, capillary electrophoresis,² and to label primers used in automated DNA sequencing.³

The spectroscopic properties of free fluorescein have been thoroughly studied,^{4,5} but less attention has been given to changes induced upon conjugation of fluorescein derivatives to macromolecules. The molar absorptivity of fluorescein has been reported to drop

Correspondence to: Mikael Kubista
Contract grant sponsor: Swedish Natural Science Research Council
Biopolymers, Vol. 46, 445–453 (1998)
© 1998 John Wiley & Sons, Inc.

by about one third upon conjugation to DNA,⁶ and the fluorescence quantum yield to drop by 26% when a fluorescein-labeled oligonucleotide is hybridized with its complementary strand.⁷ The protolytic equilibrium constants relating the mono- and dianion of fluorescein attached to various tRNA,⁸ and to the protein histone H5,⁹ have also been determined. However, there has, to date, been no systematic study of the spectroscopic and chemical properties of such complexes, which is required for quantitative studies.

In this work, we characterize the properties of fluorescein–DNA conjugates. We determine absorption, fluorescence excitation and fluorescence emission spectra, molar absorptivities, and fluorescence quantum yields of fluorescein attached to single- and double-stranded oligodeoxyribonucleotides of various lengths and sequences. We also determine the pK_a relating the fluorescein monoanion–dianion equilibrium, and find it reflects the local electrostatic potential at the nucleic acid.

MATERIALS AND METHODS

Fluorescein was purchased from Sigma, and fluorescein isothiocyanate (FITC) and tetramethyl rhodamine isothiocyanate (TRITC) from Molecular Probes, Inc. All oligodeoxyribonucleotides (Table I) were synthesized on an Applied Biosystems 380B DNA synthesizer using standard phosphoramidite chemistry with an amino group attached through a hexylcarbon linker at the 5'-end (ABI Aminolink 2) or at the 3'-end (Glen Research 3'-Amino-Modifier C7 CPG; Figure 1). FITC and TRITC were attached to the DNA according to a previously published procedure,¹⁰ except that the reaction was carried out in 0.2M carbonate buffer (pH 10). Excess dye was removed by size exclusion chromatography on a Sephadex G-25 column eluted with 0.1M NH_4Ac . All oligonucleotides and oligonucleotide–dye conjugates were purified on a 20% denaturing polyacrylamide gel, electroeluted, and then precipitated in ethanol. To ascertain that there were equal amounts of both strands in the double-stranded samples the duplexes were

Table I Oligonucleotide Sequences

Name	Sequence
9W	5'-CTA CTC GAT-3'
9C	5'-ATC GAG TAG-3'
12W	5'-CTA CCT TTC GAT-3'
12C	5'-ATC GAA AGG TAG-3'
15W	5'-CTA CCT GCA TTC GAT-3'
15C	5'-ATC GAA TGC AGG TAG-3'
18W	5'-CTA CCT GCA GAA TTC GAT-3'
18C	5'-ATC GAA TTC TGC AGG TAG-3'

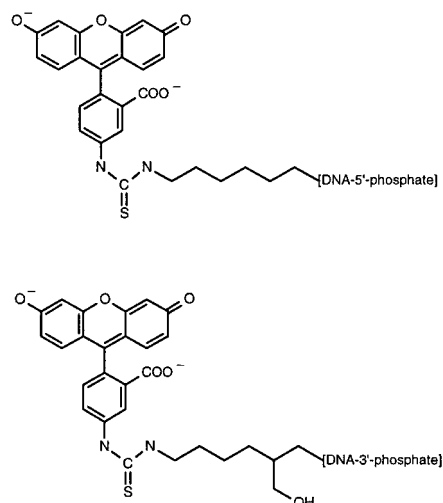


FIGURE 1 Chemical structure of the fluorescein moiety of oligonucleotide-5'-fluorescein (top) and oligonucleotide-3'-fluorescein (bottom).

purified on a 20% native polyacrylamide gel, electroeluted, and ethanol precipitated.

The DNA analogue PNA, which has the sugar–phosphate backbone replaced by uncharged N-(2-aminoethyl)glycine units,¹¹ was a gift from Professor Peter Nielsen at the Panum Institute in Copenhagen. It had the sequence H-aha-TTC TTC TTT T-NH₂, reading from the carboxy- to the amino-terminal, where H-aha is an amino-hexyl-alkyl linker that can react with FITC. Fluorescein was attached to the PNA using the same procedure as was used with the DNA, and the PNA–fluorescein conjugate was purified by extensive dialysis first against 0.1M NaCl and then against water.

Fluorescein-5'-thiourea (FI-NH₂) was made by adding 5 μ L of 5M NH_4Ac to 40 μ L of 10 mg/mL FITC in dimethyl sulfoxide (DMSO). After 10 min, another 5 μ L of 5M NH_4Ac was added and the reaction mixture was left at room temperature over night. The sample was then diluted 20 times using DMSO and purified by high performance liquid chromatography. This gave one clearly separated main product (FI-NH₂) that was evaporated to dryness and dissolved in water.

The protolytic equilibrium constants and absorption profiles of the fluorescein–DNA conjugates were determined using chemometric analysis of a set of absorption spectra recorded at different pH as described elsewhere.^{12,13} Fluorescence excitation profiles were determined from a set of excitation spectra recorded at different emission wavelengths, and the emission profiles were determined from a set of emission spectra recorded at different excitation wavelength, by Procrustes rotation analysis using the DATAN program.^{5,14,15}

Fluorescence quantum yields of FI-NH₂ and of the fluorescein–DNA conjugates were determined in 10 mM $Na_2CO_3/NaHCO_3$, pH 8.8, relative to free fluorescein in 0.1M NaOH, which was assumed to have a quantum yield of 0.93.^{16–18}

All absorption measurements were done on a Cary4 spectrophotometer using 1 cm path length and a spectral bandwidth of 1 nm. The fluorescence measurements were done in a square 1-cm cell on a Spex FL122 τ 2 spectrofluorometer. In all fluorescence measurements, the absorption was below 0.05 to minimize the inner-filter effect.¹⁹ Fluorescence lifetimes were determined by the phase-modulation technique using a scattering solution as reference, which was assumed to have zero lifetime.

RESULTS

Protolytic Equilibrium Constants and Absorption Profiles

Fluorescein exists in several protolytic forms. Around neutral pH the mono- and dianionic species are present and they have quite different spectroscopic properties. The monoanion absorbs at 453 and 472 nm and has moderate fluorescence, while the dianion absorbs at 490 nm and is intensively fluorescent.⁵ In applications at physiological pH it is therefore important to know the protolytic equilibrium constant that relates their concentrations. We have determined the protolytic equilibrium constant for several single-stranded (ss) and double-stranded (ds) fluorescein-modified oligonucleotides between 9 and 18 bases in lengths. They were synthesized in pairs of complementary strands, denoted W and C (Table I), and fluorescein was attached to the 5'-end of either of them (Figure 1). This way we could form two duplexes of the same length, where the sequence closest to the fluorescein was different. In a few cases, fluorescein was also attached to the oligonucleotide 3'-end.

The protolytic constant and the absorption profiles of the mono- and dianion of fluorescein were determined by chemometric analysis of a set of absorption spectra recorded at different pH.¹² The result obtained for oligonucleotide 9W with fluorescein attached to the 5'-end, is shown in Figure 2. The top graph shows the recorded absorption spectra, the middle graph shows the calculated concentrations of the fluorescein mono- and dianion (symbols) and the concentrations predicted by the equilibrium expression (lines), and the bottom graph shows the calculated absorption profiles of the fluorescein mono- (dashed line) and dianionic (solid line) species. The profiles were essentially identical to those of free fluorescein but for red shifts of about 6.5 (monoanion) and 3.5 (dianion) nm. The protolytic equilibrium constant was 7.11.

The pK_a values and absorption profiles for the other fluorescein–oligonucleotide conjugates were determined accordingly, and the results are summa-

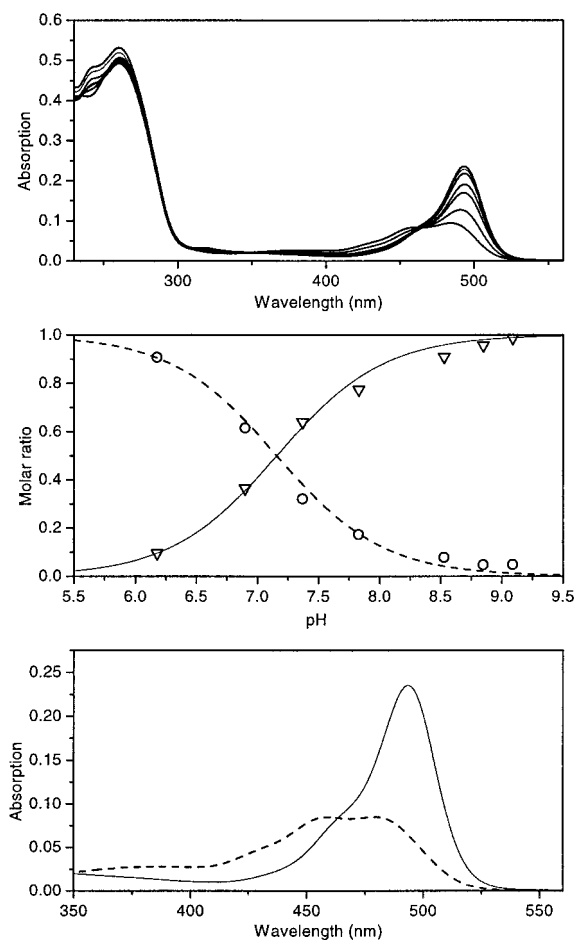


FIGURE 2 Top: Absorption spectra of FI-oligo9W in 50 mM Tris-HCl buffer at pH 6.18, 6.90, 7.37, 7.83, 8.53, 8.85, and 9.09. Middle. Calculated concentrations of FI-oligo9W mono- (○) and dianion (▽) and concentrations predicted by the determined pK_a (lines). Bottom: Calculated spectral profiles of FI-oligo9W mono- (----) and dianion (—).

rized in Table II. The protolytic equilibrium constant was not affected by the oligonucleotide length and did not depend on whether the DNA was single or double stranded. In all cases, the pK_a was close to 6.90, except for fluorescein attached to the shortest oligonucleotides (9 bases/base pairs), where it was 7.11 for the single strand and 7.02 for the duplex.

The spectral shift of the fluorescein dianion increased with increasing oligonucleotide length, being 3.5 nm for the single-stranded 9-mer and 5.6 nm for the double-stranded 18-mer. The monoanion, on the other hand, showed no systematic change in shift with oligonucleotide length. The smallest shift (4.9 nm) was observed for the single-stranded 12-mer, and the largest shift (6.8 nm) for the double-stranded 12-mer. The average spectral shift of the fluorescein species was 5.3 nm. It was somewhat larger for the monoan-

Table II Properties of Fluorescein–Oligonucleotide Conjugates

Oligonucleotide Type	Bases or Base Pairs	pK _a	Fluorescence Quantum Yield ^a	Redshift of Absorption (nm)	
				Monoanion	Dianion
Free fluorescein	—	6.43	0.93	0	0
FL-NH ₂	—	6.44		2	1
PNA	10	6.46		4	2.2
ss DNA	9	7.11	0.63(W), 0.68(C)	6.5	3.5
	12	6.90	0.27(W), 0.61(W3)	4.9	4.6
	15	6.92	0.72(W), 0.61(C) 0.52(W3), 0.54(C3)	6.3	4.7
ds DNA	9	7.02		5.3	4.3
	12	6.89	0.27(C)	6.8	5.2
	15	6.90	0.17(W)	5.8	5.5
	18	6.88	0.12(W), 0.33(C)	5.8	5.6

^a W or C indicates if the dye is attached to the W- or C-strand (Table I); 3 indicates that the dye is attached to the 3'-end, otherwise 5'.

ion (average 5.9 nm) than for the dianion (average 4.8 nm), and also larger for double-stranded (average 5.5 nm) than for single-stranded (average 5.1 nm) oligonucleotides.

The effect of the chemical modification of the carboxyphenolic ring of fluorescein upon attachment to the oligonucleotide was studied by reacting FITC with ammonium acetate. This produces fluorescein-5'-thiourea (FI-NH₂), which is characterized in Figure 3. The spectra of its protolytic species and the pK_a (6.44) are practically identical to those of free fluorescein (6.43).⁵

To test the effect of oligonucleotide charge, we attached fluorescein to the DNA analogue PNA, which is built up by the same nucleotide bases as DNA but has an uncharged backbone.¹¹ The pK_a of FI-PNA was 6.46, which is not very different from that of free fluorescein and FI-NH₂ (Table II).

Molar Absorptivities

It is far from trivial to determine the concentrations of fluorescein–oligonucleotide conjugates. It is not correct to assume that the absorption at 260 nm reflects the concentration of the oligonucleotide, since fluorescein also has substantial absorption in the uv region,¹² and this contribution is unknown. We have used another way to determine the concentrations of fluorescein-labeled oligonucleotides. In addition to the fluorescein-labeled oligonucleotide, we synthesized the complementary oligonucleotide labeled with tetramethyl-rhodamine. With these two strands, and the corresponding unlabeled ones, we could form four duplexes: one labeled with fluorescein (F), one labeled with tetramethyl-rhodamine (R), one doubly

labeled (FR), and one unlabeled (U). The concentration of U was determined from its absorption at high temperature, where the oligonucleotides have lost all secondary structure and the absorptivity is the sum of the contributions from the individual nucleotides:

$$\varepsilon_{260} = n_G \cdot 11.7 + n_C \cdot 7.3 + n_A \cdot 15.4 + n_T \cdot 8.8 \text{ (mM}^{-1} \text{ cm}^{-1}\text{)} \quad (1)$$

ε_{260} is the molar absorptivity of the oligonucleotide at 260 nm and n_X is the number of bases of type X.²⁰ Assuming

$$\varepsilon_{FR}(\lambda) = \varepsilon_F(\lambda) + \varepsilon_R(\lambda) - \varepsilon_U(\lambda) \quad (2)$$

the concentrations of F, R, and FR were determined relative to U by fitting the absorption spectra of the four oligomers according to Eq. (3) (Figure 4).

$$A(\lambda)_{FR} = k_F \cdot A(\lambda)_F + k_R \cdot A(\lambda)_R + k_U \cdot A(\lambda)_U \quad (3)$$

where $A(\lambda)_i$ are the absorption spectra of the oligomers and k_i are fitting parameters that can be expressed as the concentration ratios $k_F = c_{FR}/c_F$, $k_R = c_{FR}/c_R$ and $k_U = -c_{FR}/c_U$. Since c_U is known, the concentrations of the other oligomers can also be calculated. This was done for six samples with oligonucleotide lengths of 12, 15, and 18 base pairs that had fluorescein attached to the 5'-end of either the W- or C-strand. At pH 7.46 the molar absorptivity of conjugated fluorescein was $51200 \pm 1400 \text{ M}^{-1} \text{ cm}^{-1}$ at its absorption maximum (494 nm), and for conjugated tetramethyl-rhodamine it was $89600 \pm 1100 \text{ M}^{-1} \text{ cm}^{-1}$ (556 nm).

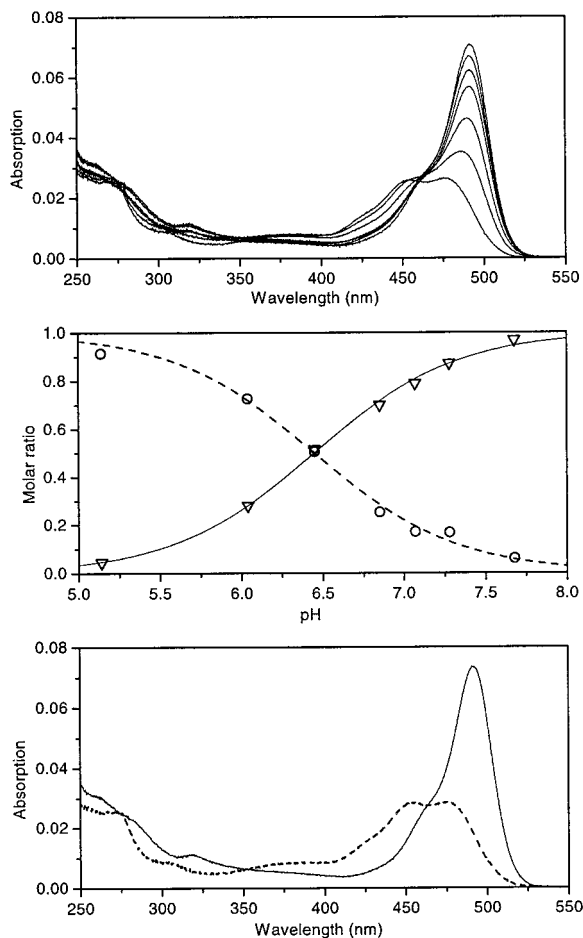


FIGURE 3 Top: Absorption spectra of FI-NH₂ in 10 mM phosphate buffer at pH 5.14, 6.04, 6.45, 6.85, 7.06, 7.28, and 7.68. Middle: Calculated concentrations of FI-NH₂ mono- (○) and dianion (▽) and concentrations predicted by the determined pK_a (lines). Bottom: Calculated spectral profiles of FI-NH₂ mono- (-----) and dianion (—).

Fluorescence Quantum Yields

The fluorescence quantum yields of the fluorescein dianion attached to the oligonucleotides were determined relative to free fluorescein (Table II). The quantum yields varied considerably, but were in all cases substantially lower than the quantum yield of free fluorescein (0.93).^{16–18} At 25°C, the lowest quantum yield (0.12) was observed for fluorescein attached to oligo18W in the duplex form, and the largest quantum yield (0.72) was observed for fluorescein attached to single-stranded oligo15W.

For all oligomers the fluorescence quantum yield decreased with increasing temperature. This is shown in Figure 5 for oligo12W, whose quantum yield decreases from 0.27 at 1°C to 0.18 at 80°C. The measurement was done at a pH (8.8) high enough for the

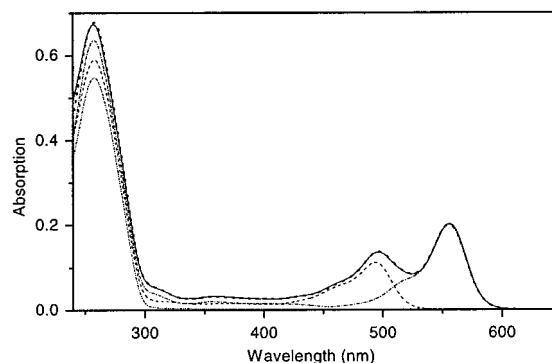


FIGURE 4 Absorption spectra of a 15-base pairs oligonucleotide duplex labeled with fluorescein (-----), with tetramethyl rhodamine (- · - · -), with both fluorescein and tetramethyl rhodamine (—), unlabeled (- · · · · -), and the best fit of F, R, and U to FR (· · · · ·). Spectra were measured in 30 mM Tris, 20 mM NaCl, and 1 mM EDTA at pH 7.46.

dianion of fluorescein to totally dominate, and the decrease in quantum yield was not an effect of shifting the protolytic equilibrium. The redshift of the absorption spectrum with increasing temperature (Figure 5, inset, and Ref. 5) was taken into account when calculating the quantum yields. A similar decrease in fluorescence quantum yield was observed for other fluorescein-modified oligomers studied, while free fluorescein did not show this dependence on temperature (data not shown).

To test if protein binding affected the fluorescence quantum yield of fluorescein–DNA conjugates, we added the recombination protein RecA. This protein polymerizes onto DNA until it covers the entire oligonucleotide (see, for instance, Ref. 21). When added to

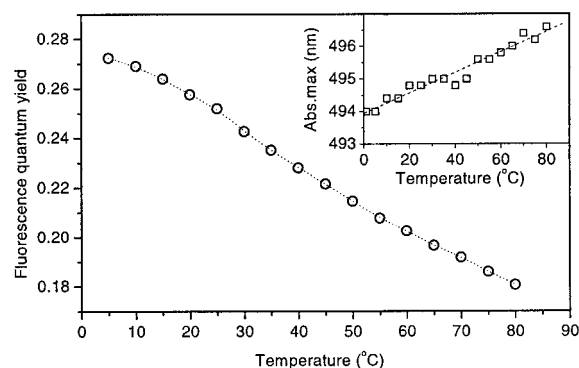


FIGURE 5 Fluorescence quantum yield of FI–oligo12W as a function of temperature. Spectra were measured in 10 mM carbonate buffer at pH 8.8. Quantum yields are corrected for temperature variations in absorption. Inset: Wavelength of absorption maximum as a function of temperature.

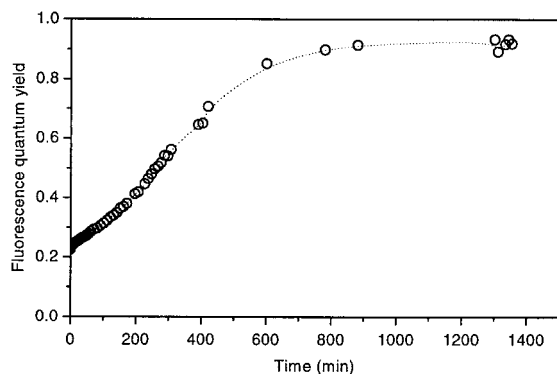


FIGURE 6 Increase in fluorescence quantum yield of fluorescein-labeled 12 base pairs duplex upon addition of RecA protein. Sample contained $0.5 \mu\text{M}$ oligomer duplex, $2.6 \mu\text{M}$ RecA, 20 mM phosphate buffer (pH 7.53), 50 mM NaCl, 4 mM MgCl_2 , and $40 \mu\text{M}$ $\text{ATP}\gamma\text{S}$.

the double-stranded fluorescein-modified 12-mer, the quantum yield increased more than fourfold, becoming as high as the quantum yield of free fluorescein (Figure 6).

Fluorescence Lifetimes

The FI-DNA conjugates have complex fluorescence decay. Under all conditions, including high pH where only the dianion is present, at least double exponential decays were observed. This is different from free fluorescein, which at high pH has a single exponential lifetime of 4.1 ns .⁵ The fluorescence lifetimes were independent of temperature. For FI-oligo12W at pH 8.8, they were 3.8 ± 0.1 and $1.2 \pm 0.3 \text{ ns}$ between 20 and 50°C . Their relative contributions however, varied. The preexponential factor of the long-lifetime component decreased from 0.84 at 20°C to 0.74 at 50°C .

Fluorescence Excitation and Emission Profiles

Figure 7(top) shows excitation spectra of FI-oligo15W recorded using different emission wavelengths at pH 6.18 (left) and pH 7.17 (right). By chemometric analysis the excitation spectra (bottom left) of the monoanionic (dashed line) and dianionic (solid line) species, as well as the emission intensities at the emission wavelengths used (bottom right, symbols) were calculated.^{5,14} Corresponding analysis of emission spectra is shown in Figure 8. The excitation and emission profiles of conjugated fluorescein are essentially identical to those of free fluorescein,⁵ except that there was a spectral shift to longer wave-

length of about 5 nm . The responses for the oligomer in duplex form were the same (not shown).

DISCUSSION

Using fluorescein as a probe for protein binding,²² DNA hybridization, and ligand binding,²³ in fluorescence energy transfer measurements,¹ etc., requires detailed knowledge about the spectroscopic and chemical properties of fluorescein-nucleic acid conjugates. We have characterized several conjugates, which will hopefully provide a base for such applications. Further, we show that when these properties are known, the local electrostatic potential around the nucleic acid can be estimated from the spectra of the conjugated fluorescein.

The Protolytic Equilibrium is Shifted Toward the Monoanion

For fluorescein conjugated to nucleic acids, the pK_a is about 6.90 (Table II). This is considerably higher than

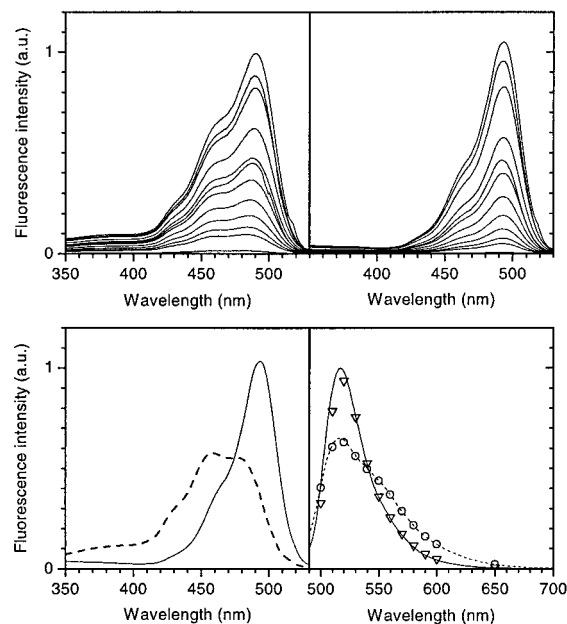


FIGURE 7 Fluorescence excitation spectra of FI-oligo15W at pH 6.18 (top left) and at pH 7.17 (top right) measured using emission wavelengths 510, 520, 530, 540, 550, 560, 570, 580, 590, 600, and 650 nm. Bottom left: Calculated fluorescence excitation profiles of FI-oligo15W mono- (---) and dianion (—). Bottom right: Calculated intensities at the emission wavelengths used of mono- (\circ) and dianion (∇), compared to the emission spectra determined in Figure 8 (lines). The pH was adjusted using 10 mM phosphate buffer.

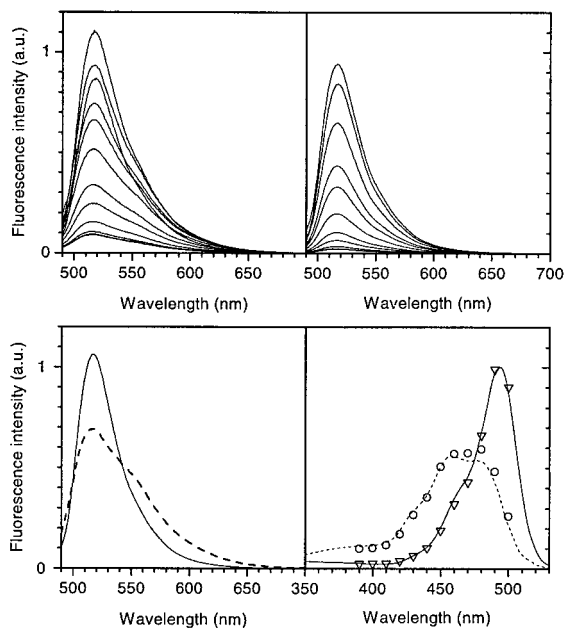


FIGURE 8 Fluorescence emission spectra of FI-oligo15W at pH 6.18 (top left) and at pH 7.17 (top right) measured using excitation wavelengths 390, 400, 410, 420, 430, 440, 450, 460, 470, 480, 490, and 500 nm. Bottom left: Calculated fluorescence emission profiles of FI-oligo15W mono- (---) and dianion (—). Bottom right: Calculated intensities at the excitation wavelengths used of mono- (○) and dianion (▽), compared to the excitation spectra determined in Figure 7 (lines). The pH was adjusted using 10 mM phosphate buffer.

for free fluorescein, which has a pK_a of 6.43.⁵ Several effects may contribute to this difference. The negative electrostatic potential around the polyanionic DNA is expected to repel the dianion more than the monoanion, which should shift the equilibrium toward the monoanion, hence increasing the pK_a . Both the covalent modification of the carboxyphenylic moiety of fluorescein, and stacking interaction between the xanthene ring system of fluorescein and the nucleic acid bases, may also affect the pK_a .

To test the effect of the covalent modification we studied FI-NH₂, which is fluorescein chemically modified as in the fluorescein–oligonucleotide conjugates. Its pK_a was 6.44, which is essentially the same as for free fluorescein (6.43). Clearly, the chemical modification has no effect on the pK_a in accordance with previous findings that substitutions on the carboxyphenyl ring hardly affect the spectroscopic properties of fluorescein.²⁴

The effect of attachment was studied using the uncharged DNA analogue PNA. The pK_a of FI-PNA was 6.46 (Table II), which is only slightly larger than that of free fluorescein. Hence, if fluorescein stacks

with the nucleic acid bases it only marginally effects the pK_a . Since neither chemical modification of fluorescein nor its attachment to an uncharged nucleic acid base polymer has significant effect on its pK_a , we conclude that the shift of fluorescein pK_a upon covalent attachment to DNA is caused by the electrostatic potential of the phosphate backbone.

Probing the Local Electrostatic Potential

We find no essential difference when comparing the protolytic equilibrium constants of fluorescein–nucleic acid conjugates in single- and double-stranded form (Table II). This implies that there is no major difference between the potential around single- and double-stranded oligonucleotides. Although one may intuitively think that the electrostatic potential should be larger around double-stranded than around single-stranded DNA, our results are in agreement with theoretical predictions based on the counterion condensation theory.²⁵ Record et al. have estimated that there are effectively 0.76 monovalent cations associated with each phosphate in double-stranded DNA, and about 0.44 with each phosphate in single-stranded DNA.^{26,27} This results in a net charge of $-0.48e$ per base pair in double-stranded DNA and $-0.56e$ per base in single-stranded DNA. Hence, the theory even predicts a somewhat more negative electrostatic potential around single-stranded oligonucleotides. Interestingly, for the oligonucleotides we have studied we find a somewhat higher pK_a for single strands than for duplexes, in agreement with this prediction (Table II).

The local electrostatic potential ψ around the DNA is given by²⁸

$$\begin{aligned} \psi &= -[R \cdot T \cdot \ln 10 / (N_A \cdot e)] \cdot \Delta pK_a \\ &= -59.2 \cdot \Delta pK_a \text{ (mV) (at } 25^\circ\text{C)} \quad (4) \end{aligned}$$

where ΔpK_a is the difference between the pK_a in the presence and absence of the electrostatic potential, R is the universal gas constant, T is the absolute temperature in K, N_A is the Avogadro constant, and e is the elementary charge. For modified oligonucleotides of at least twelve bases, irrespective of whether they are single or double stranded, the pK_a is about 6.90. For free fluorescein, the pK_a is 6.43.⁵ This gives $\Delta pK_a = 0.47$, which corresponds to an effective electrostatic potential of -28 mV. For the 9-mers the pK_a is about 7.06, corresponding to $\psi \approx -37$ mV.

The fluorescein moiety is attached to the DNA via a six-carbon linker and a thiourea bond, which are flexible and about 10–15 Å in length. Its distance from the DNA is therefore not well defined. The rms

end separation of a polyethylene chain is on average $l \cdot \sqrt{2} \cdot \sqrt{N}$, where N is the number of C—C bonds and l is the bond length.²⁹ In our case this corresponds to about 5–7 Å. However, it should be considered a lower limit, since both protolytic species are negatively charged, and repelled by the nucleic acid.

Our finding that the fluorescein pK_a is independent of oligonucleotide length above 12 bases/base pairs, implies that the electrostatic potential is fully developed at this length. This is considerably shorter than expected from Monte Carlo simulations of counterion distribution, which predict that the concentration of cations at the oligonucleotide end increases up to about 24 bases.³⁰

Fluorescein Absorption is Reduced by Conjugation to Nucleic Acids

We determined the molar absorptivity of fluorescein–oligonucleotide conjugates to $51000M^{-1} \text{ cm}^{-1}$ at 494 nm and pH 7.46. At this pH, both the fluorescein mono- and dianion are present, and the pK_a relating their concentrations is 6.90 (Table II). Hence, at pH 7.46, 72% of the fluorescein is dianion and 28% is monoanion. This allows us to normalize the spectral responses determined in Figure 2, giving a molar absorptivity of $62,000M^{-1} \text{ cm}^{-1}$ at 494 nm for the dianion, and of $23,000M^{-1} \text{ cm}^{-1}$ at 478 (and 459) nm for the monoanion. In previous studies, only effective molar absorptivities at particular pH values were determined. Clegg et al.⁶ obtained $46,000M^{-1} \text{ cm}^{-1}$ at pH 8.3, and Mergny et al.³¹ obtained $36,000M^{-1} \text{ cm}^{-1}$ at pH 7.0. Assuming $pK_a = 6.90$ these determinations correspond to $48,000M^{-1} \text{ cm}^{-1}$ and $56,000M^{-1} \text{ cm}^{-1}$ for the fluorescein dianion. Both values are somewhat lower than those we obtained, which we believe is because they determined the concentrations of the fluorescein–DNA conjugates from the uv absorption underestimating the fluorescein contribution. It is clear, though, that the molar absorptivities of both the fluorescein mono- and dianion in the conjugates are considerably lower than those of free fluorescein ($29,000$ and $76,900M^{-1} \text{ cm}^{-1}$ at maximum absorption for the mono- and dianion, respectively).⁵

Above pH 5, the fluorescein mono- and dianion are the only fluorescein species present. From their molar absorptivities and the pK_a of 6.90 for oligomers of at least twelve bases/base pairs, it is possible to determine the concentration of fluorescein–oligonucleotide conjugates by absorption. At 494 nm, which is the wavelength of maximum absorption of the dianion, the molar absorptivity of the fluorescein monoanion is

$12000M^{-1} \text{ cm}^{-1}$, which gives a total molar absorptivity of the fluorescein–nucleic acid conjugate of

$$\varepsilon_{494}(\text{pH}) = 62,000/[1 + 10^{-(\text{pH}-6.90)}] + 12,000/[1 + 10^{(\text{pH}-6.90)}](M^{-1} \text{ cm}^{-1}) \quad (5)$$

Fluorescence Quantum Yield Depends on Temperature, Environment, and Oligonucleotide Length, Sequence, and Conformation

The fluorescence quantum yield of the conjugated fluorescein dianion depends on the oligonucleotide length, its sequence, where the dye is attached (3' or 5' end), and also on the oligonucleotide conformation. For double-stranded oligonucleotides, we found quantum yields between 0.17 and 0.33, while for the single-stranded ones, with the exception of oligonucleotide 12W, the quantum yields were between 0.52 and 0.72. Clearly, double-stranded nucleic acids seem to reduce the quantum yield of fluorescein to a much larger extent than single-stranded ones. For FI-oligo12W the quantum yield was only 0.27. At present we do not know the reason for its low fluorescence efficiency. It has been suggested that fluorescein may interact sequence specifically with DNA,^{32,33} which could affect the fluorescence. However, we do not think this is the reason for the low fluorescence of FI-oligo12W since the oligonucleotides in each series (W or C) have the same terminal sequence and FI-oligo12W is the only one with divergent fluorescence.

The fluorescence quantum yield of fluorescein–oligonucleotide conjugates decreases with increasing temperature (Figure 5). We have ruled out that this is due to increasing amounts of monoanionic fluorescein, since the measurements were done at pH 8.8 where essentially all fluorescein is present as dianion, which was also verified by absorption measurements. It must therefore be due to a decrease in quantum yield of the dianion. The addition of RecA protein to fluorescein–oligonucleotide conjugates increases the fluorescence severalfold, reaching a level similar to that of free fluorescein (Figure 6). This implies that the reduced fluorescence quantum yield of fluorescein–oligonucleotide conjugates is not due to the covalent attachment, but is caused by some noncovalent interaction between the fluorescein and the nucleic acids.

The temperature dependence of the quantum yield, the effect of protein binding and also the biexponential fluorescence decay of conjugated fluorescein dianion (Table II), suggest that fluorescein–oligonucle-

otide conjugates exist in at least two conformational states, each with a different quantum yield. The less luminescent conformation is favored by duplex formation and high temperature, hence having higher entropy, and it may be disrupted by protein binding.

We thank Professor Peter Nielsen at the Panum Institute in Copenhagen for supplying PNA. The work was supported by the Swedish Natural Science Research Council.

REFERENCES

- Clegg, R. M., Murchie, A. I., Zechel, A. & Lilley, D. M. J. (1993) *Proc. Natl. Acad. Sci. USA* **90**, 2994–2998.
- Smith, L. M., Sanders, J. Z., Kaiser, R. J., Hughes, P., Dodd, C., Connell, C. R., Heiner, C., Kent, S. B. H. & Hood, L. E. (1986) *Nature* **321**, 674–679.
- Cheng, Y. & Dovichi, N. J. (1988) *Science* **242**, 562–564.
- Lindqvist, L. (1960) *Ark. Kemi* **16**, 79–138.
- Sjöback, R., Nygren, J. & Kubista, M. (1995) *Spectrochim. Acta Part A* **51**, L7–L21.
- Clegg, R. M., Murchie, A. I. H., Zechel, A., Carlberg, C., Diekmann, S. & Lilley, D. M. J. (1992) *Biochemistry* **31**, 4846–4856.
- Cardullo, R. A., Agrawal, S., Flores, C., Zamecnik, P. C. & Wolf, D. E. (1988) *Proc. Natl. Acad. Sci. USA* **85**, 8790–8794.
- Friedrich, K., Woolley, P. & Steinhäuser, G. (1988) *Eur. J. Biochem.* **173**, 231–239.
- Favazza, M., Lerho, M. & Houssier, C. J. (1990) *Biomol. Struct. Dynam.* **7**, 1291–1300.
- Agrawal, S., Christodoulou, C. & Gait, M. J. (1986) *Nucleic Acid Res.* **14**, 6227–6245.
- Egholm, M., Nielsen, P. E., Burchardt, O. & Berg, R. H. (1992) *J. Am. Chem. Soc.* **114**, 9677–9678.
- Kubista, M., Sjöback, R. & Albinsson, B. (1993) *Anal. Chem.* **65**, 994–998.
- Kubista, M., Sjöback, R. & Nygren, J. (1995) *Anal. Chim. Acta* **302**, 121–125.
- Kubista, M. (1990) *Chem. Int. Lab. Sys.* **7**, 273–279.
- Scarmino, I. & Kubista, M. (1993) *Anal. Chem.* **65**, 409–416.
- Weber, G. & Teale, F. W. J. (1957) *Trans. Faraday Soc.* **53**, 646–655.
- Hercules, D. M. & Frankel, H. (1960) *Science* **131**, 1611–1612.
- Seybold, P. G., Gouterman, M. & Callis, J. (1969) *Photochem. Photobiol.* **9**, 229–242.
- Kubista, M., Sjöback, R., Eriksson, S. & Albinsson, B. (1994) *Analyst* **119**, 417–419.
- Sambrook, J., Fritsch, E. F. & Maniatis, T. (1989) in *Molecular Cloning: A Laboratory Manual*, 2nd ed., Cold Spring Harbor Laboratory Press, Cold Spring Harbor, NY, p. 11.30.
- Kubista, M., Simonson, T., Sjöback, R., Widlund, H. & Johansson, A. (1996) in *Biological Structure and Dynamics*, Vol. 1, Sarma, R. H. & Sarma, M. H., Eds., Adenine Press, NY, pp. 49–59.
- Houston, P. & Kodadek, T. (1994) *Proc. Natl. Acad. Sci. USA* **91**, 5471–5474.
- Muramaki, M., Nakaura, M., Nakatsuji, Y., Nagahara, S., Tran-Cong, Q. & Makino, K. (1991) *Nucleic Acid Res.* **19**, 4097–4102.
- Fabian, W. M. F., Schuppler, S. & Wolfbeis, O. S. (1996) *J. Chem. Soc. Perkin Trans. 2*, 853–856.
- Manning, G. S. (1969) *J. Chem. Phys.* **51**, 924–933.
- Record, M. T., Jr., Woodbury, C. P. & Lohman, T. M. (1976) *Biopolymers* **15**, 893–915.
- Anderson, C. F., Record, M. T., Jr. & Hart, P. A. (1978) *Biophys. Chem.* **7**, 301–316.
- Friedrich, K. & Woolley, P. (1988) *Eur. J. Biochem.* **173**, 227–231.
- Atkins, P. W. (1990) in *Physical Chemistry*, 4th ed., Oxford University Press Oxford, pp. 701–702.
- Olmsted, M. C., Anderson, C. F. & Record, M. T., Jr. (1989) *Proc. Natl. Acad. Sci. USA* **86**, 7766–7770.
- Mergny, J.-L., Bourtoune, A. S., Garestier, T., Belloc, F., Rougée, M., Bulychev, N. V., Koshkin, A. A., Bourson, J., Lebedev, A. V., Valeur, B., Thuong, N. T. & Hélène, C. (1994) *Nucleic Acid Res.* **22**, 920–928.
- Millar, D. P., Hochstrasser, R. A., Guest, C. R. & Chen, S. M. (1992) *SPIE Proc. Intl. Soc. Opt. Eng.* **1640**, 592–598.
- Kumke, M. U., Shu, L., McGown, L. B., Walker, G. T., Pitner, J. B. & Linn, C. P. (1997) *Anal. Chem.* **69**, 500–506.